Journal of Physics: Conference Series

PAPER • OPEN ACCESS

Distortion prevention of axisymmetric parts during laser metal deposition

To cite this article: P A Golovin *et al* 2018 *J. Phys.: Conf. Ser.* **1109** 012065

IOP Conf. Series: Journal of Physics: Conf. Series **1109** (2018) 012065 doi:10.1088/1742-6596/1109/1/012065

Distortion prevention of axisymmetric parts during laser metal deposition

P A Golovin[1, 2], A M Vildanov[1, 2], K D Babkin[1, 2], S Y Ivanov[1, 2] and I K Topalov[1, 2]

[1] Institute of Laser and Welding Technologies, Peter the Great St. Petersburg Polytechnic University, St. Petersburg, 195251, Russia
[2] St. Petersburg State Marine Technical University, St.Petersburg, 190121, Russia

E-mail: golovinp2015@gmail.com

Abstract. One of the main problem of large parts manufacturing using laser metal deposition (LMD) is the high residual distortion. Effects of layer-by-layer evolution of stresses and strains was studied by finite-element simulation. It was shown that distortion of axially symmetrical parts can be successfully predicted by the developed simulation procedure. Required dimensional accuracy of additively manufactured parts can be achieved by the optimization of deposited part size and shape in order to compensate volume shrinkage during layers solidification. The corresponding simulation procedure was developed and validated. Another major problem is prevention of distortion during deposition of thick flange on the surface of thin shell structures. In this case the following procedure was proposed and studied: on the first step spacer ring introduces in the shell, then deposition of the flange is carried out and on the last stage whole structure is heat treated in order to remove residual stresses.

1. Introduction

Every year, engineers are developing ever more complex mechanisms and parts of machines to increase their efficiency and productivity, optimize the shape and materials used, however, this affects the increase in the laboriousness of production of such products, for example, aircraft engines or devices from the aerospace industry. Moreover, the overall dimensions of engines used in aircraft construction are quite large and can reach 3 meters in diameter with a wall thickness of several centimeters. The production of engine casings is a complex and time-consuming task, so rapidly developing additive technologies seek to solve and simplify the task of manufacturing such parts [1-5].

In particular, Institute of Laser and Welding Technologies (ILWT), Peter the Great St.Petersburg Polytechnic University was tasked to produce a prototype of the gas turbine engine support made of titanium alloy, a diameter of more than 800 mm with a wall thickness of 3 mm and thick flange – about 15 mm – on it. However, this presents some difficulties, due to the process of metal melting and its further crystallization, as is known, leads to the appearance of internal stresses into the part and its deformation. Therefore, we put forward two hypotheses: in the case the product is produces without supports, the product itself must have sufficient rigidity to has internal stresses resistance during the manufacture, whereby cracks on the product and its destruction are avoided; In the case where the product cannot retain internal stresses without deformation or failure, we need to use supporting structures. We have developed and applied an innovative way to add extra rigidity to a thin-walled structure using internal supporting structures. The point of this approach is that the body of the necessary shape and size is first made, then a special support device is inserted into it, the so-called spacer pan, which adds extra rigidity to the construction and prevents the destruction of a thin-walled product, after which the flanges and other elements are grown on the surface of the housing. Next, it is necessary to make a heat treatment of the product, remove the special support device and send the product to the final treatment.

Both hypotheses were tested, the results of the study compared with the results of the simulation, the data were analyzed, based on it, a decision on the possibility of producing large-sized thin-walled parts from titanium alloys using laser metal deposition (LMD) technology with and without supporting structures and on distortion prevention of axisymmetric parts were made.

2. Experimental part

The experiments were carried out using ILWT's laser metal deposition setup (Figure 1).

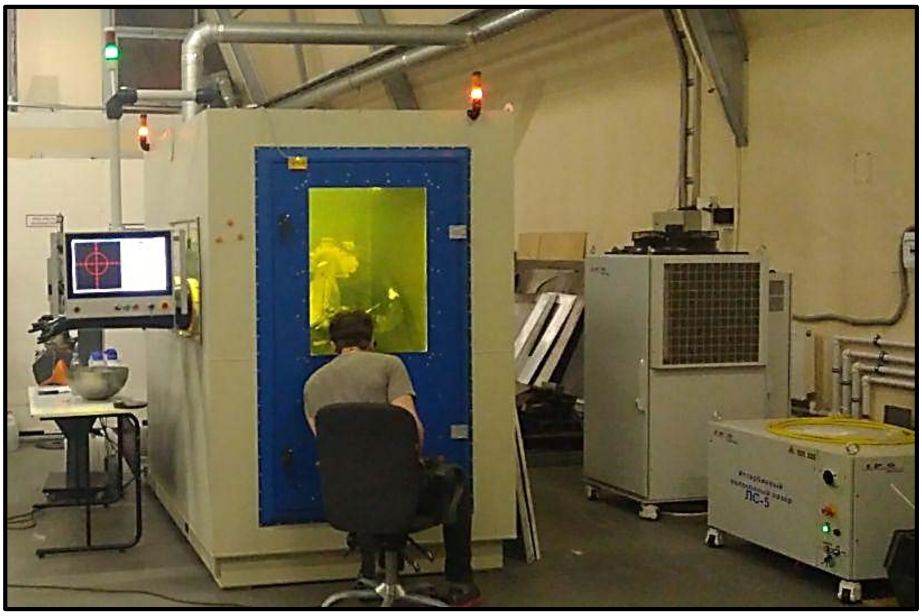

Figure 1. Laser metal deposition setup with an operator.

It consist of the following main parts:

- a 5 kW fiber laser IPG LS-5 coupled with chiller Riedel PC 160;
- a powder feeder Oerlikon Twin 10-C;
- a six-axis robot manipulator Fanuc coupled with a two-axis positioner Fanuc;
- a welding laser head IPG FLW-D30 with a coaxial slit nozzle;
- a sealed chamber of a 6 m^3 volume with the possibility of obtaining an argon atmosphere with a purity of ≈ 100 ppm oxygen content.

A series of three trials was carried out using this setup:

1) Thin-walled cylinder of IN625 on the substrate of low-alloy steel. There are scheme and appearance of this part on Figure 2. It was deposited on the following process parameters:

- Laser power: 1.5 kW;
- Deposition rate: 30 mm s^{-1};
- Beam radius: 1.2 mm;
- Number of layers: 246;
- Cylinder radius: 100 mm.

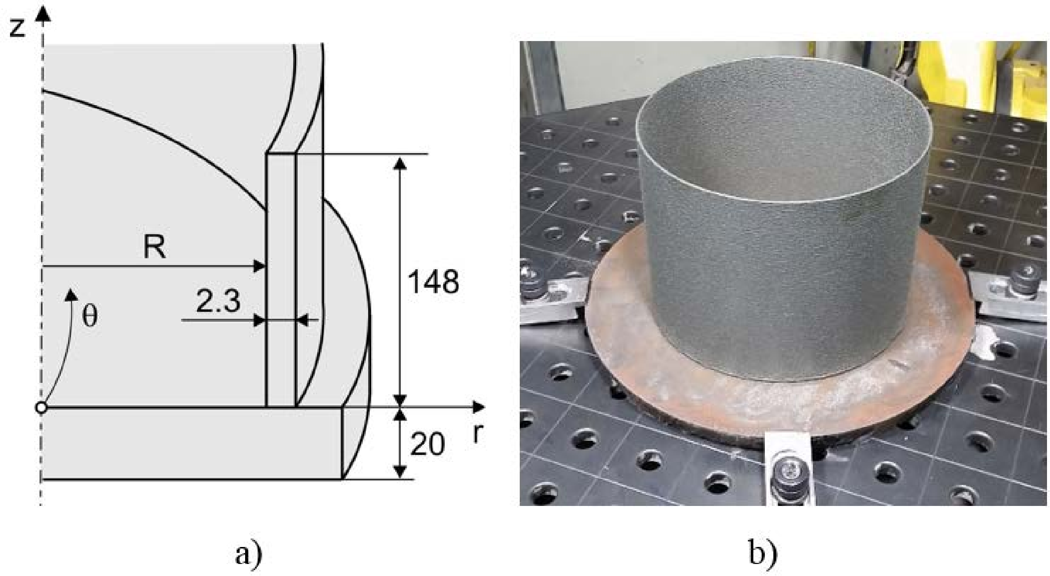

Figure 2. Schematic (a) and photo (b) of the deposited cylinder of IN625.

2) Thin-walled cylinder of Ti-6Al-4V on the substrate of the same alloy. There is a scheme of this part on Figure 3. It was deposited in 100 % argon atmosphere on the following process parameters:

- Power: 1.6 kW;
- Deposition rate: 30 mm s^{-1};
- Beam radius: 1.2 mm;
- Number of layers: 600;
- Cylinder radius: 420 mm.

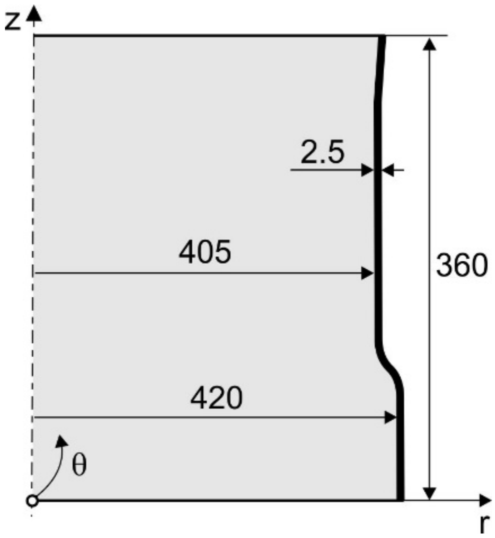

Figure 3. Scheme of the deposited cylinder of Ti-6Al-4V

Subsequently residual distortion of the build parts was measured by the Shining 3D EinScan-Pro laser scanner and Geomagic software was used for data processing. Due to the comparison of the geometric dimensions of the theoretical model and the manufactured product, the first hypothesis was partially disproved: large-sized products have sufficient rigidity to resist internal stresses, but the latter cause unacceptably large deformations. Therefore, it is necessary to use supporting structures to impart extra rigidity to thin-walled structures.

3) Thin-walled cylinder of Ti-6Al-4V with thick flanges on the substrate of the same alloy. There is an appearance of this part on Figure 4. Based on the previous trials and simulation data it was decided to produce the part in two steps: build the thin-walled cylinder using optimised deposition path at first; insert extra-rigid supports, which pushes to outside, into the cylinder and deposit thick flanges on cylinder side. It was deposited in 100 % argon atmosphere on the following process parameters:

   - Power: 2.3 kW;
   - Deposition rate: 20 mm/s;
   - Beam radius: 1.75 mm;
   - Wall thickness: 4.2 mm;
   - Flange thickness: 10 mm.

Figure 4. Photo of the deposited cylinder of Ti-6Al-4V with flanges

Residual distortion of the build part was also measured by the Shining 3D EinScan-Pro laser scanner and Geomagic software was used for data processing.

3. Simulation part

The sequentially-coupled heat conduction analysis in transient mode followed by elastic-plastic large displacement analysis has been performed using finite element method. Deposition of material during LMD was simulated using so-called element birth technique. In this method, elements for the yet to be deposited are deactivated at the beginning and then gradually activated of “born” into the solution domain (Figure 5). Finite element model of deposited parts was 2D axisymmetric. The temperature-dependent mechanical properties for IN625 [6] and Ti-6Al-4V [7] was used in Figure 6.

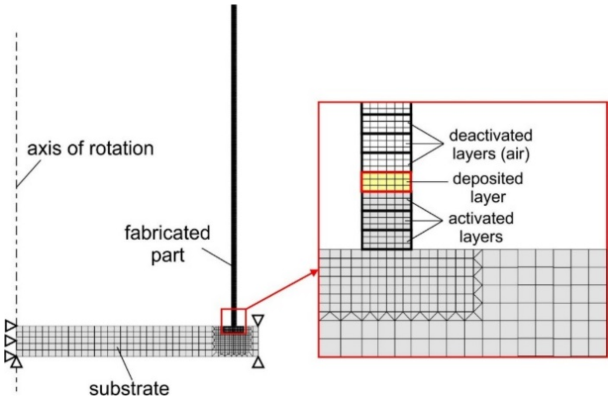

Figure 5. FE mesh and mechanical boundary conditions

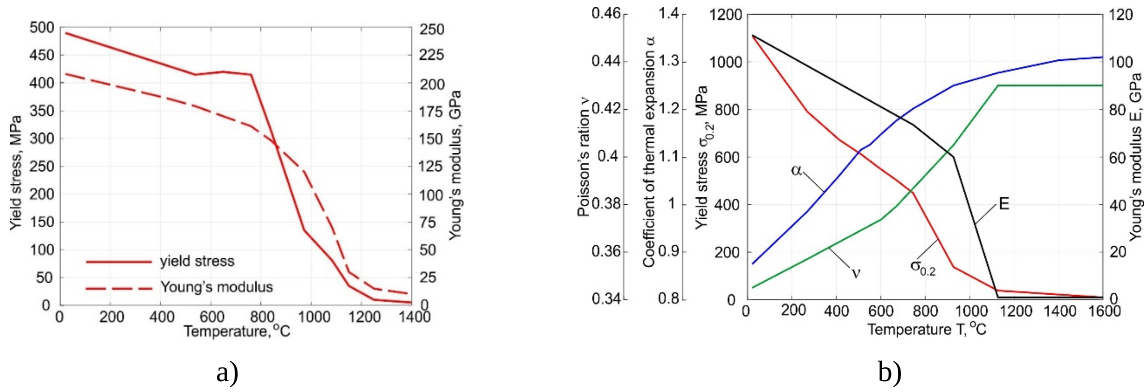

Figure 6. Temperature-dependent mechanical properties for IN625 (a) and Ti-6Al-4V (b).

4. Results and discussion

4.1. Residual stress and distortion of the deposited cylinder of IN625

Effects of radius variation of the deposited cylinder on distortion and temperature field along the cylinder generator of a constant height are shown in Figure 7. As can be seen, the effect of increasing cylinder radius is to increase residual radial displacement and curvature of the sidewall. It can be explained by a large amount of the deposited metal in one layer due to higher circumference on the one hand and the lower thermal gradient along sidewall on the other. Colder metal prevents the temperature expansion of the solidify deposited layer and leads to the generation of higher shortening plastic stain and thus higher distortion. The lower radius, the greater temperature gradient and the peak temperature before the deposition of the current layer. It leads to the more uniformly shrinkage and less warping.

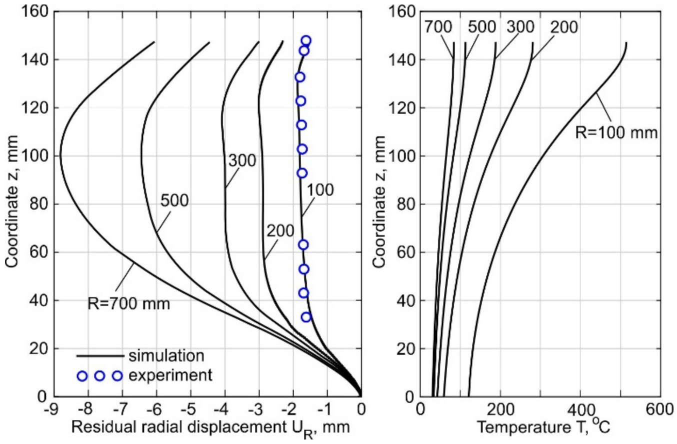

a) b)

Figure 7. Residual radial displacement along the cylinder generator as a function of cylinder radius (a); Temperature distribution along the cylinder generator before the deposition of the last layer (b).

Analysis of residual stresses in build cylinder of 700 mm radius revealed that the highest tension hoop and axial stress amounted to (1.15-1.2)$\sigma_{0.2}$ near the substrate (Figure 8a, b). It can be explained by the high stiffness of the substrate and increasing in bending moment with increased wall height. It was also revealed that axial plastic strain is tension and attains 1.5-2.0% (Figure 8c). This leads to the conclusion that if deposited material has a weak ductility (e.g. titanium alloys) there is a high probability that the fracture could occur in this region. Residual radial stress is neglectfully small due to thin sidewall of the cylinder.

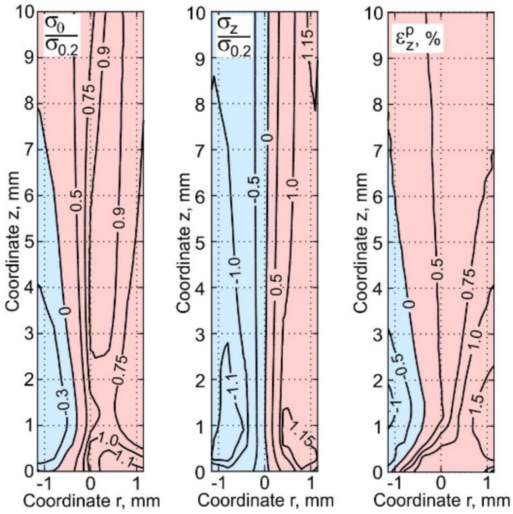

a) b) c)

Figure 8. Distribution of normalised hoop stress (a), normalised axial stress (b) and axial plastic strain (c) in the sidewall cross section of the cylinder of 700 mm radius.

4.2. Analysis of distortion of Ti-6Al-4V cylinder

During the first experimental trial deposition path completely agree with part generator shown in Figure 3. Measured mismatch along generator between build part and required shape is shown in Figure 9. It can be seen that deviation is negative and amounted to about 5 mm, that is unacceptable. The next experimental trial was carried out according to the optimised deposition path obtained by the numerical simulation. In this case, the peak mismatch amounted 1 mm only on the small area of the part whereas an average deviation is only 0.2 mm (Figure 9b).

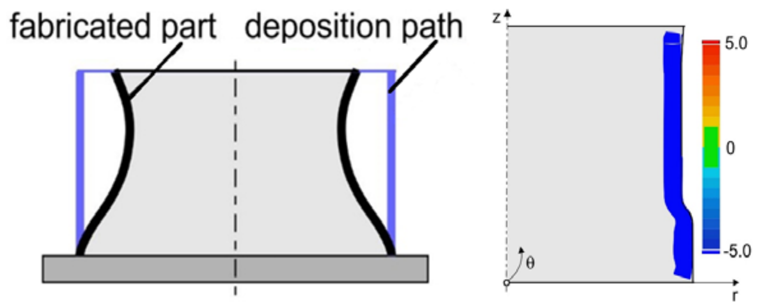

a) b)

Figure 9. Scheme of fabrication part deviation from deposited part (a) and distribution of mismatch between required model and build part obtained using non-optimised deposition path (b)

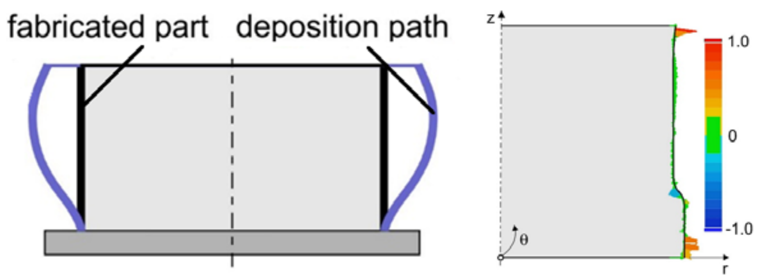

a) b)

Figure 10. Scheme of fabrication part deviation from deposited part (a) and distribution of mismatch between required model and build part obtained using optimised deposition path (b)

4.3. Analysis of distortion of Ti-6Al-4V cylinder with thick flanges

Cause of non-uniform residual distortion and heat influence on the built cylinder during flanges cladding unexpected deviation were appeared and registered. Despite of optimised deposition path and extra-rigid supports the deviation were significant, although at the support-mounted places distortion were the least.

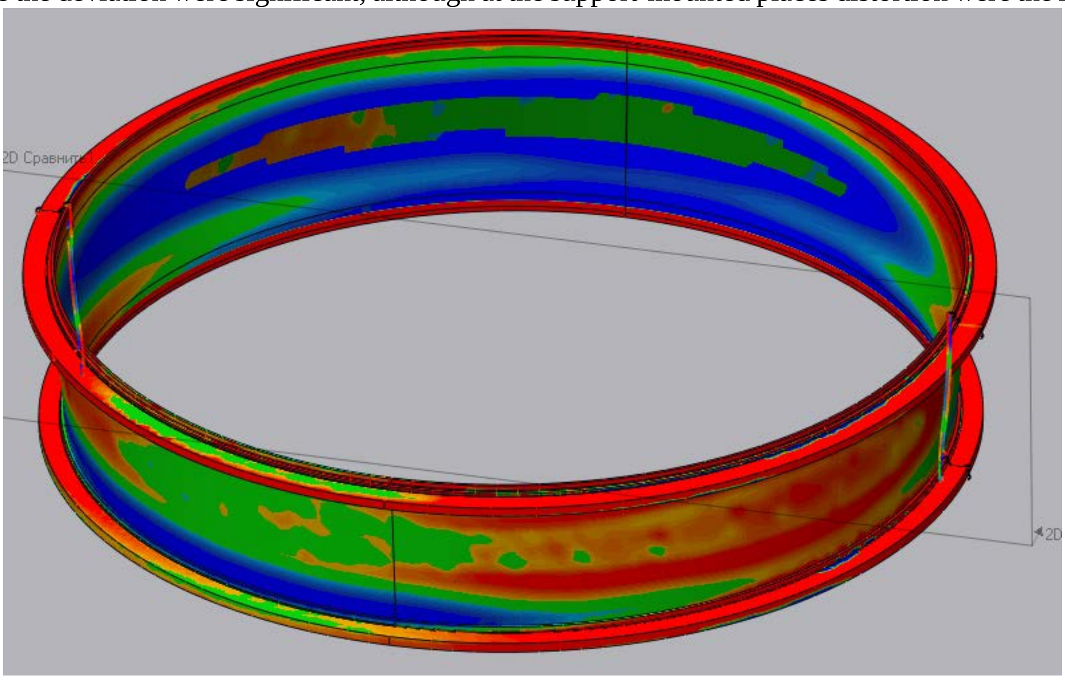

Figure 11. Distribution of mismatch between required model and build part obtained using optimised deposition path**.**

5. Conclusions

1) The effect of increasing cylinder radius is to increase residual radial displacement and curvature of the sidewall.
2) The highest tension hoop and axial stress amounted to 1.15-1.2 times of yield stress near the substrate.
3) If deposited material has a weak ductility (e.g. titanium alloys) there is a high probability that the fracture could occur in the sidewall near the substrate.

Acknowledgements
The work was carried out with financial support from the Ministry of Education and Science of the Russian Federation. (Unique project ID: RFMEFI57417X0175).

References

[1] Gu D D, Meiners W, Wissenbach K, Poprawe R 2012 *Int. Mat. Rev.* **57** 133-64.
[2] Sames W J, List F A, Pannala S, Dehoff R R, Babu S S 2016 *Int. Mat. Rev.* **61** 315-60.
[3] Turichin G A, Somonov V V, Babkin K D, Zemlyakov E V, Klimova O G 2016 *IOP Conf. Ser.: Mat. Sci. and Eng.* **125** 012009.
[4] Klimova-Korsmik O, Turichin G, Zemlyakov E, Babkin K 2016 *Phys. Proc.* **83** 716-22.
[5] Turichin G, Zemlyakov E, Babkin K, Ivanov S, Vildanov A 2018 *Proc. CIRP* **74** 154–57.
[6] High-temperature high strength nickel base alloys. Nickel Development Institute 1995;393.
[7] Cao J, Gharghouri M A, Nasha P 2016 *J. Mat. Proc. Tech.* **237** 409–19.

Journal of Physics: Conference Series

PAPER • **OPEN ACCESS**

A simplified model for numerical simulation of laser metal deposition process with beam oscillation

To cite this article: S Y Ivanov *et al* 2018 *J. Phys.: Conf. Ser.* **1109** 012006

A simplified model for numerical simulation of laser metal deposition process with beam oscillation

S Y Ivanov[1,2], A Artinov[3], E A Valdaytseva[1,2], S L Stankevich[1,2], G A Turichin[1]

[1] St. Petersburg State Marine Technical University, St. Petersburg, 190121, Russia
[2] Institute of Laser and Welding Technologies, Peter the Great St. Petersburg Polytechnic University, St. Petersburg, 195251, Russia
[3] BAM Federal Institute for Materials Research and Testing, Berlin, 12205, Germany

E-mail: sergei.yu.ivanov@gmail.com

Abstract: A model of laser metal deposition with beam oscillation has been developed. The proposed model consists of two coupled sub-models calculating the heat transfer in the deposited part and the free surface of the molten pool, respectively. The heat transfer simulation of the deposited part solves a three-dimensional quasi-stationary heat conduction problem. The free surface of the molten pool are determined by solving the Laplace-Young equation. The developed model enables the layer-by-layer prediction of the shape of the deposited part and the resulting temperature field. It is shown that for an oscillation amplitude equal to the beam radius the peak value of the heat flux decreases by about 53% and 73% in the case of lateral oscillation and circular oscillation, respectively. Lateral oscillating laser beam results in a higher penetration depth due to the higher thermal efficiency. The amplitude of the laser beam oscillation effects the shape of the deposited wall and the deposition rate. A good correlation between the numerically calculated and experimentally observed results is obtained.

1. Introduction

The laser metal deposition (LMD) is an advanced manufacturing technology, which enables the production of complex parts of higher dimensions and partially or completely eliminate the need for the machining and welding [1-4]. The use of the LMD as an everyday industrial tool is still prevented by the high number of process parameters which influence the quality of the deposited parts. A development of an optimal process parameters requires a lot of expensive experimental trials. For this reason, numerical simulation is used to reduce the number of experiments and hence to improve the quality and efficiency of the process. The state of the art numerical models in the field of LMD consider only the physical phenomena during the deposition of a limited number of layers [5-7]. Due to the long computational times, such models are well suited for optimizing the LMD process, by investigating its influencing factors. On the other hand, there are simplified models based on analytical solutions and empirical relations [8, 9]. These models offer lower accuracy and are used for a rough prediction of the temperature field during deposition of the first layer.

Using beam oscillation during welding and brazing a reduction of the porosity, an increase of the gap bridging ability and the process efficiency are obtained [10, 11]. The deposition rate of a LMD process can also be increased by modifying the size and shape of the molten pool through beam oscillation [12]. Another positive effect is the decrease of the waviness of the surface of the deposited wall. It is especially important in the case of a titanium alloys, which are widely used for the production of thin-walled components. These alloys, e.g. Ti-6Al-4V, offer a high corrosion resistance and find an application in the aerospace industry. Nevertheless their machining is challenging due to the low thermal conductivity and sticking phenomena.

The aim of the present work is to develop a simplified model for the numerical simulation of the laser metal deposition process with beam oscillation. Hereby the precise and fast prediction of the shape of the deposited parts and the temperature field during the process is the focus of this investigation.

2. Mathematical model

2.1.1. Simulation procedure

Since the physics of laser processing are strongly coupled and strongly nonlinear, the equations used for the modelling of the laser metal deposition must be simplified in order to guarantee numerical stability and fast computational time. The thermophysical material properties play a crucial role in the modelling of the temperature field and the fusion zone. The material properties used in the simulation are summarized in Figure 1 [13]. The flowchart of the multi-physics simulation can be seen in Figure 2. Here, the solver sequences used to obtain the solution for a single layer are presented. The sequentially-coupled quasi-stationary heat conduction analysis followed by the calculation of the static free surface problem are performed using the finite difference method (FDM). For this simulation, the developed in-house code is implemented using the commercial programming language MATLAB.

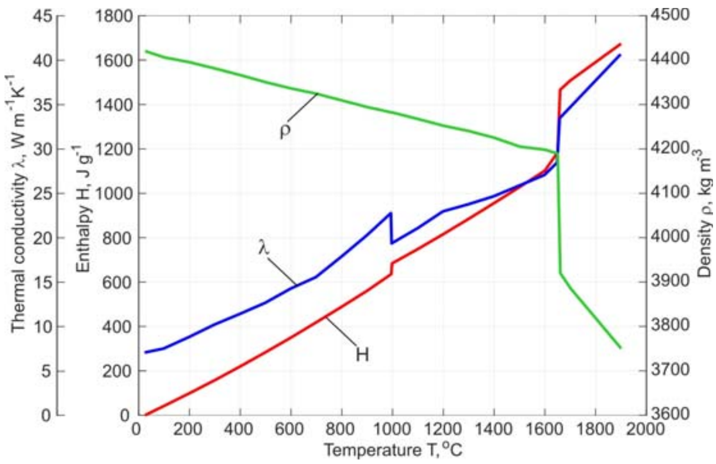

Figure 1. Thermophysical properties of Ti-6Al-4V used in the model.

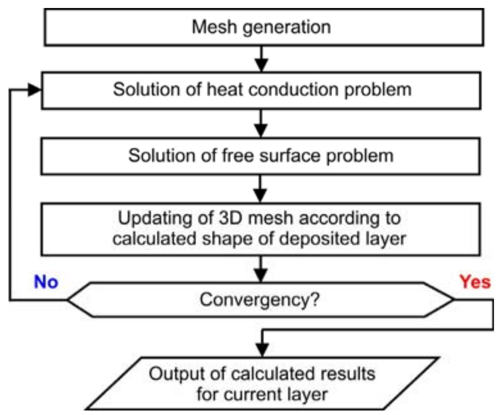

Figure 2. Flowchart of the multi-physics simulation used for the calculation of a single layer.

2.1.2. Heat conduction problem

In order to improve the stability and the computational time of the model, the following assumptions are made:

- non-stationary phenomena at the beginning and the end of a deposited layer are neglected
- vaporization and radiation are not considered
- thermophysical properties are known functions of the temperature, see Figure 1.

Under the assumptions made, the formulation of the nonlinear quasi-stationary in Cartesian coordinates becomes:

$$\frac{\partial}{\partial x}\left(\lambda\frac{\partial T}{\partial x}\right)+\frac{\partial}{\partial y}\left(\lambda\frac{\partial T}{\partial y}\right)+\frac{\partial}{\partial z}\left(\lambda\frac{\partial T}{\partial z}\right)+vc\rho\frac{\partial T}{\partial x}+q_3=0\,, \tag{1}$$

where λ is the thermal conductivity, $c\rho$ is the volumetric heat capacity, v is the scanning speed and q_3 is the volumetric heat source power.

The boundary conditions at the top surface of the calculation domain are the following:

$$-\lambda\frac{\partial T}{\partial z}=q_{2L}(x,y)\,. \tag{2}$$

Here q_{2L} is the heat flux of the laser beam.

First-order boundary conditions i.e. temperature distribution are applied at the bottom surface and the side surfaces. The temperature field is calculated according to the well-known analytical solution presented in [14].

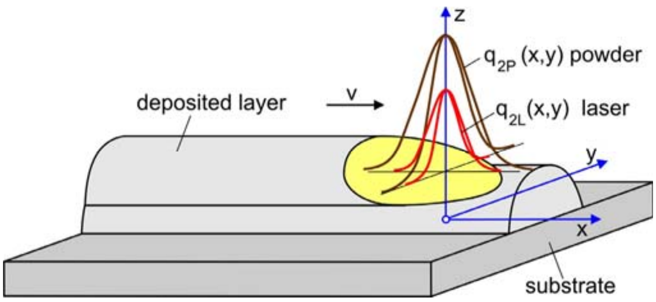

Figure 3. Schematic of the computational domain and the reference frame.

2.1.3. A heat source model for an oscillating laser beam

The normally distributed heat flux of the laser beam without oscillation is defined by the peak value of the heat flux and the laser beam radius:

$$q_2(x,y)=q_{2m\ n}\exp\left(-\frac{x^2+y^2}{R_b^2}\right), \tag{3}$$

$$q_{2m\ n}=\frac{\eta\cdot q}{\pi\cdot R_b^2},$$

where $q_{2m\ n}$ is the peak value of heat flux and R_b is the normal radius of heat source.

In the case of an oscillating laser beam the heat flux distribution depends not only on the previously discussed parameters but also on additional parameter related to the oscillation amplitude. The heat flux of the oscillating laser beam, see Figure 4 and 5, can be mathematically represented by the following equations:

- for lateral oscillated laser beam:

$$q_2(x,y)=\begin{cases} q_{2\max}\exp\left(-\dfrac{x^2+y^2}{R_b^2}\right) & if\ \ |y|\geq A \\ q_{2\max}\exp\left(-\dfrac{x^2}{R_b^2}\right) & if\ \ |y|<A \end{cases} \tag{4}$$

- for circular oscillated laser beam:

$$q_2(r) = \frac{q_{2\max}}{2}\left\{\exp\left[-\frac{(A-r)^2}{R_b^2}\right] + \exp\left[-\frac{(A+r)^2}{R_b^2}\right]\right\} \tag{5}$$

$$r = \sqrt{x^2 + y^2} \ ,$$

Here $q_{2\max}$ is the peak value of heat flux and A is the oscillation amplitude.

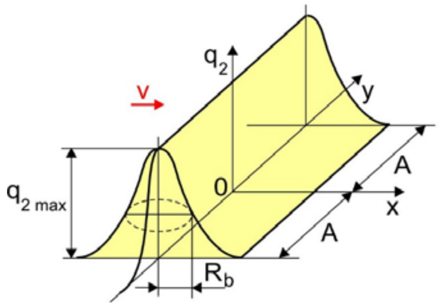

Figure 4. Heat flux distribution of lateral oscillated laser beam.

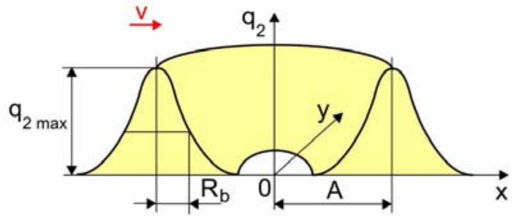

Figure 5. Heat flux distribution of circular oscillated laser beam.

The effective heat power of the heat source q_e can be evaluated as follows:

$$q_e = \eta \cdot q = \eta \cdot \int_{-\infty}^{+\infty}\int_{-\infty}^{+\infty} q_2(x,y)dxdy \tag{6}$$

where η is the heat source efficiency and q is the heat source power. The process efficiency depends on numerous factors such as material of substrate, surface preparation and local temperature field. The temperature dependent efficiency is used according to experimental data [15].

Substituting equations (4) and (5) into eq. (6) and representing the oscillation amplitude as a function of the laser beam radius $A = n \cdot R_b$ the peak value of the heat flux is obtained:

- for lateral oscillated laser beam:

$$q_{2\max} = q_{2m\ n} \cdot \frac{\sqrt{\pi}}{\sqrt{\pi} + 2 \cdot n} = q_{2m\ n} \cdot k_A \tag{7}$$

- for circular oscillated laser beam:

$$q_{2\max} = q_{2m\ n} \cdot \frac{1}{\exp(-n^2) + n \cdot \sqrt{\pi} \cdot erfc(-n)} = q_{2m\ n} \cdot k_A \ . \tag{8}$$

The coefficient k_A can be used to analyze the effects of the oscillating amplitude on the heat flux density, see Figure 6. By setting the parameter n to one the amplitude will be equal to the laser beam radius. In this case the peak of the heat flux decreases by about 53% by lateral and 73% by circular oscillation of the laser beam, respectively. An increase of the amplitude leads to an increase of the weld pool width and length and a decrease of the penetration depth, see Figure 7. Note, that the lateral oscillating laser beam has a higher penetration depth due to the higher thermal efficiency.

IOP Conf. Series: Journal of Physics: Conf. Series **1109** (2018) 012006 doi:10.1088/1742-6596/1109/1/012006

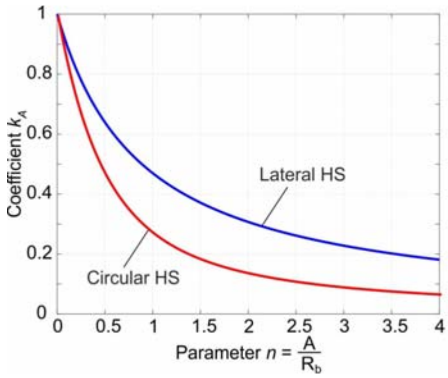

Figure 6. Coefficient k_A as a function of parameter n.

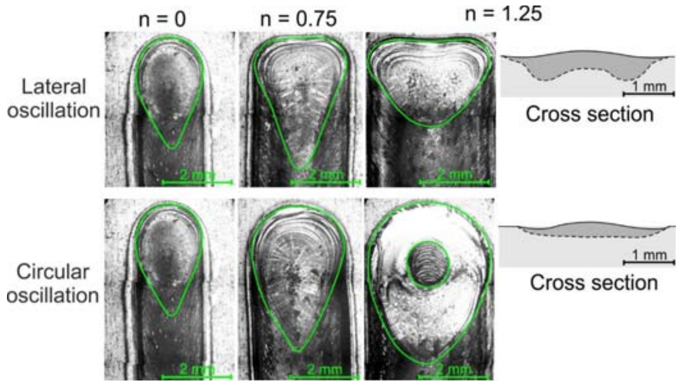

Figure 7. Effect of the oscillation amplitude on the molten pool shape.

2.1.4. Free surface calculation

The equilibrium equation of the liquid phase in the gravity field can be used to predict the cross section of the deposited layer. This equation links the curvature of the free surface of the molten pool and the surface tension by the hydrostatic pressure, see Figure 8 [16]:

$$\sigma\ \kappa = -\rho\ g\ z_o + C \tag{9}$$

where σ is the surface tension, κ is the curvature of the free surface, ρ is the density, g is gravity constant and C is the Lagrange multiplier.

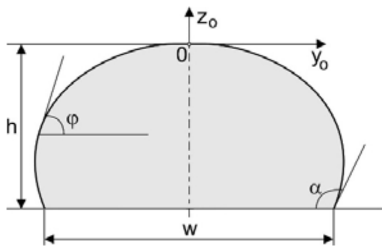

Figure 8. Schematic of the free surface shape of the deposited layer.

The cross-sectional shape of the deposited layer described by the curve $y_o = f(z_o)$ can be defined as follows:

$$\kappa = \frac{f''}{\left(1+f'^2\right)^{3/2}} = \frac{1}{f'}\left(\frac{1}{1+f'^2}\right)' . \tag{10}$$

A parametric form of the curve can be given as:

$$\begin{cases} z_o = z_o(\varphi) \\ y_o = y_o(\varphi) \end{cases} \quad 0 \le \varphi \le \alpha . \tag{11}$$

After manipulations, the following system of ordinary differential equations is obtained:

$$\begin{cases} \dfrac{dz_o}{d\varphi} = \dfrac{\sin\varphi}{B} \\ \dfrac{dy_o}{d\varphi} = -\dfrac{\cos\varphi}{B} \end{cases} \tag{12}$$

where $B = \dfrac{\rho\ g\ z_o}{\sigma} + C$.

The boundary conditions for the obtained ODEs is the following:

1) $z_o(0) = 0;\ y_o(0) = 0$
2) $y_o(-h) = 0.5w$,

where w is the width of the molten pool.

3) $2\int_{-h}^{0} y_o dz_0 = S_{lay}$,

where h is the calculated height of the deposited layer and S_{lay} is the area of the deposited layer.

The area of the deposited layer is the sum of areas of the melted substrate and the deposited per unit time filler material. The latter can be determined by integrating the mass flux of the gas-powder jet over the molten pool surface. The powder flux distribution can be described by the following expression:

$$q_{2P}(x,y) = \frac{q_P}{\pi\ r_P^2}\exp\left[-\frac{x^2+y^2}{r_P^2}\right], \tag{13}$$

where q_P is the mass flow of powder and r_P is the effective radius of the gas-powder jet.

The desired shape of the deposited layer is determined by the previously calculated molten pool width, the area of the deposited metal and the Lagrange multiplier satisfying boundary condition. The system of ODEs (12) is solved by the fourth and fifth-order and Runge-Kutta method.

3. Example

A thin Ti-6Al-4V wall was deposited by LMD process in 100% argon atmosphere onto a Ti-6Al-4V substrate. The following process parameters were used: laser power of 2.3 kW, deposition rate of 30 mm s^{-1}, beam radius of 1.5 mm, lateral beam oscillation amplitude of 1.25 mm and powder flow rate of 0.42 g s^{-1}. After the deposition of each layer, the deposited wall was cooled down natural convection and heat conduction to 60-80 ^{o}C. The average value of the surface tension of the liquid titanium alloy in the temperature range between 1670 – 1770 ^{o}C was constant and equal to 1.55 N m^{-1} [17].

A comparison of the experimentally measured and numerically calculated width of the deposited wall show good correlation and can be seen in Figure 9. A deviation is observed near the center line of the wall. This is due to the neglected convection in the molten pool and the pressure of the gas-powder stream, which are not considered in the model. The effects of the process parameters on the shape of the deposited wall and the temperature field are analyzed numerically, see Figure 10. An increase of the oscillation amplitude by about 40%, from 1.25 mm to 1.75 mm, leads to a decrease of the width of the deposited material due to the decreasing thermal efficiency of the heat source. Note here, that the deposition rate is also decreasing, due to the decreasing molten pool area and therefore deteriorating powder catchment efficiency. By reducing the oscillation amplitude by 40% practically the opposite effect is observed.

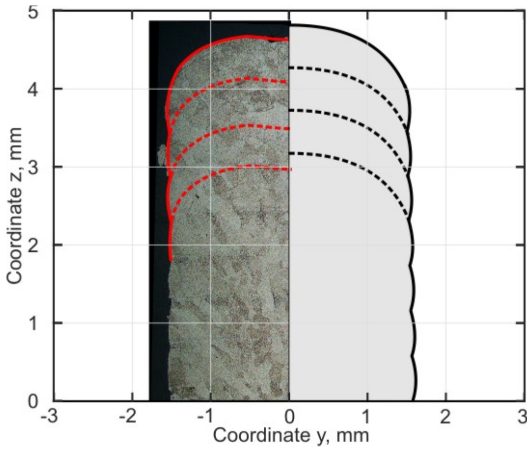

Figure 9. Experimental (left) and calculated (right) cross section of the deposited wall.

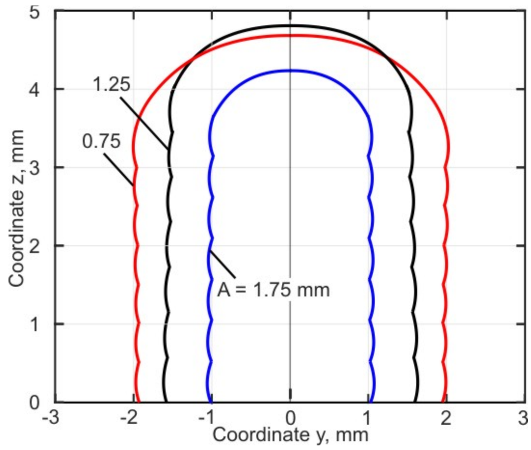

Figure 10. Effect of the amplitude of lateral oscillated laser beam on the cross section of the deposited wall.

4. Conclusions

The aim of the present investigation is to develop a simplified numerical model for the prediction of the shape the temperature field of LMD produced parts. The advantages of this approach are the reduced computation time and good accuracy.

It is shown that the oscillation amplitude has a strong influence on the value of peak heat flux. By setting the amplitude to be equal to the value of the laser beam radius the peak heat flux decreases by 53% for lateral oscillation and by 73% for circular oscillation. Lateral oscillating beam has a higher penetration depth due to higher thermal efficiency. The laser beam oscillation amplitude effects the shape of the deposited wall and the deposition rate in the process. The proposed model is used for the analysis of the effects of the process parameters on the resulted shape of the deposited wall. A good agreement between the numerical results and the experimental measurements is achieved.

Acknowledgements

The work was carried out with financial support from the Ministry of Education and Science of the Russian Federation. (Unique project ID: RFMEFI57417X0175).

References

[1] Gu D D, Meiners W, Wissenbach K, Poprawe R 2012 *Int. Mat. Rev.* **57** 133-64
[2] Sames W J, List F A, Pannala S, Dehoff R R, Babu S S 2016 *Int. Mat. Rev.* **61** 315-60
[3] Turichin G, Zemlyakov E, Babkin K, Ivanov S, Vildanov A 2018 *Proc. CIRP* **74** 184–7
[4] Klimova-Korsmik O, Turichin G, Zemlyakov E, Babkin K. 2016 *Phys. Procedia* **83** 716-22
[5] Knapp G L, Mukherjee T, Zuback J S, Wei H L, Palmer T A, De A, DebRoy T 2017 *Acta Mater.* **135** 390-99
[6] Lee Y, Farson D F 2016 *J. Laser Appl.* **28** 0120061-8
[7] Dubrov A V, Mirzade F K, Dubrov V D 2018 *J. Synch. Investig.* **12** 54-63
[8] Pinkerton A J, Li L 2004 *J. Phys. D: Appl. Phys.* **37** 1885
[9] Picasso M, Marsden C, Wagniere J, Frenk A, Rappaz M 1994 *Metall. Mater. Trans. B* **25** 281-91
[10] Müller A, Goecke S F, Rethmeier M 2018 *Weld. World* **62** 1039-1047
[11] Kraetzsch M, Standfuss J, Klotzbach A, Kaspar J, Brenner B, Beyer E 2011 *Phys. Proc.* **12** 142-149
[12] Turichin G, Zemlyakov E, Babkin K, Ivanov S, Vildanov 2018 *Proc. CIRP* **74** 154–57

[13] Mills K C 2002 *Recommended Values of Thermophysical Properties for Selected Commercial Alloys* (Cambridge: Woodhead Publishing)
[14] Nguyen N 2004 *Thermal analysis of welds* (Ashurst: WIT press)
[15] Kwon H, Baek W-K, Kim M-S, Shin W-S, Yoh J J 2012 *Opt. Lasers Eng.* **50** 114-21
[16] Landau L D, Lifshits E M 1987 *Fluid Mechanics* (Oxford: Pergamon press)
[17] Paradis P F, Ishikawa T, Yoda S 2002 *Int. J. Thermophys.* **23** 825-42

Scopus

Поиск Источники Помощь SciVal

Сведения об источнике

Отзыв > Сравнить источники >

Journal of Physics: Conference Series

Годы охвата Scopus: с 2005 по настоящий момент

Издатель: Institute of Physics Publishing

ISSN: 1742-6588 E-ISSN: 1742-6596

Отрасль знаний: Physics and Astronomy: General Physics and Astronomy

Просмотреть все документы > Настроить оповещение о документе Journal Homepage

Перейти на сайт показателей журналов Scopus

CiteScore 2017
0.48

SJR 2017
0.241

SNIP 2017
0.447

CiteScore | CiteScore рейтинг и тренды | Содержание Scopus

CiteScore 2017

Вычислено с использованием данных из 30 April, 2018

0.48 = Количество цитирований 2017 / Документы с 2014 - 2016* = Цитат: 8 561 > / 17 872 документов >

* Показатель CiteScore включает все доступные типы документов

Просмотр методики CiteScore > Часто задаваемые вопросы о CiteScore >

CiteScoreTracker 2018

Дата последнего обновления *08 December, 2018*
Ежемесячное обновление

0.42 = Количество цитирований 2018 / Документы с 2015 - 2017 = 9 149 цитирований на текущую дату > / 21 895 документов на текущую дату >

Рейтинг CiteScore

Категория	Рейтинг	Процентиль
Physics and Astronomy General Physics and Astronomy	#154/202	23-й

Просмотр трендов CiteScore > Добавить CiteScore на свой сайт

Direct Laser Deposition with Transversal Oscillating of Laser Radiation

Conference Paper · June 2018

DOI: 10.1109/LO.2018.8435626

G. A. Turichin
Peter the Great St.Petersburg Polytechnic University

E. V. Zemlyakov
Peter the Great St.Petersburg Polytechnic University

Mikhail Kuznetsov
Peter the Great St.Petersburg Polytechnic University

Artur Kurakin
State Marine Technical University

Direct Laser Deposition with Transversal Oscillating of Laser Radiation

G.A. Turichin[1], E.V. Zemlyakov[1,2], M.V. Kuznetsov[1,2], K.D. Babkin[1,2], A.I. Kurakin[1], A.M. Vildanov[1,2]

[1] Saint Petersburg State Marine Technical University, Saint Petersburg, Russian Federation

[2]Institute of Laser and Welding Technologies, Peter the Great Saint Petersburg Polytechnic University, Saint Petersburg, Russian Federation

e-mail: kuznetsov_mich@ltc.ru

***Abstract* — the objective of this research is investigation influence spot diameter, frequency and amplitude of transversal oscillating laser radiation on the efficiency and coefficient of using materials of the direct laser deposition. Efficiency and coefficient of using materials of the direct laser deposition were increased from 15 g/min up to 22.2 g/min and from 27.6% up to 44.4% accordingly at the transversal oscillating laser radiation with spot diameter 0.9 mm, frequency 100 Hz and amplitude 2.6 mm comparatively with seems indicator of the direct laser deposition with spot diameter 3.2 mm without oscillating.**

Keywords — high power fiber laser, direct laser deposition, transversal oscillating of laser radiation.

Uniform spatial distribution of laser radiation is more preferable for realization laser cladding and laser deposition because of minimal and uniform remelting zone of substrate and minimal dilution base and filler metal at the smooth appearance of the formed cladding layer [1]. Uniform spatial distribution of laser radiation at the using fiber laser can be obtained by additional module for laser head **-** «beam shaper» which transforms spatial distribution of laser radiation optically. Transversal oscillation of laser radiation can transforms Gaussian spatial distribution to uniform also. Some authors used transversal oscillation of laser radiation for achievement maximal efficiency of laser cladding process with minimal and uniform remelting zone of substrate [2].

The research is devoted to study influence of spot diameter (0.9 mm, 2 mm, 3.2 mm), frequency (from 0 Hz up to 350 Hz) and amplitude transversal oscillation of laser radiation (from 0 mm up to 2.6 mm) on the efficiency and coefficient using materials (powder) of the direct laser deposition.

Research was performed using technological laser system on the base ytterbium fiber laser LS-15. Laser head YW50 (Precitec) equipped by galvanometer scanner ILV DC-SCANNER was used. Metal powder Inconel 625 with fraction 52-150 microns was delivered to the melting zone from noncoaxial inkjet nozzle by powder feeder TWIN 10-C (Sulzer Metco).

Walls with width 3 mm, height 50 mm and roughness 50 microns were deposited. Maximal efficiency of the direct laser deposition and coefficient of using materials were received at the transversal oscillation laser radiation with frequency 100 Hz, amplitude 2.6 mm and spot diameter 0.9 mm and were 22.2 g/min and 44.4% accordingly. It was on the 48% и 61% more seems indicators of the direct laser deposition without oscillation with spot diameter 3.2 mm. The indicators increased because of uniform spatial distribution laser radiation was obtained by transversal oscillating laser radiation and minimal remelting zone was formed. Average dendrites length without oscillation was about 700 microns that more on the 15% than average dendrites length with oscillation. It can be explain because of changing of heat input and cooling speed of the thermal cycle of the deposition.

Research was performed at the support Ministry of Education and Science of Russian Federation – unique identifier of the project RFMEFI57417X0175.

REFERENCES

[1] D. Tanigawa, Yo. Funada, N. Abe, M. Tsukamoto, Yos. Hayashi, H. Yamazaki, Yo. Tatsumi, M. Yoneyama, "Suppression of dilution in Ni-Cr-Si-B alloy cladding layer by controlling diode laser beam profile," Optics and Laser Technology, vol. 99, 2018, pp. 326–332.

[2] J. Tuominen, J. Näkki, H. Pajukoski, T. Peltola, P. Vuoristo, M. Kuznetsov, E. Pozdeeva, E. Zemlyakov, G. Turichin "Laser cladding with 15 kW fiber laser", Proceeding of the 13th Nolamp Conference, 2011, pp. 1-12.

Сведения о документе

Proceedings - International Conference Laser Optics 2018, ICLO 2018
13 August 2018, Номер статьи 8435626, Page 214
2018 International Conference Laser Optics, ICLO 2018; St. Petersburg; Russian Federation; 4 June 2018 до 8 June 2018; Номер категорииCFP1836X-ART; Код 138711

Direct laser deposition with transversal oscillating of laser radiation (Conference Paper)

Turichin, G.A.[a], Zemlyakov, E.V.[a,b], Kuznetsov, M.V.[a,b], Babkin, K.D.[a,b], Kurakin, A.I.[a], Vildanov, A.M.[a,b]

[a]Saint Petersburg State Marine Technical University, Saint-Petersburg, Russian Federation
[b]Institute of Laser and Welding Technologies, Peter the Great Saint Petersburg Polytechnic University, Saint-Petersburg, Russian Federation

Краткое описание

Просмотр пристатейных ссылок (2)

The objective of this research is investigation influence spot diameter, frequency and amplitude of transversal oscillating laser radiation on the efficiency and coefficient of using materials of the direct laser deposition. Efficiency and coefficient of using materials of the direct laser deposition were increased from 15 g/min up to 22.2 g/min and from 27.6% up to 44.4% accordingly at the transversal oscillating laser radiation with spot diameter 0.9 mm, frequency 100 Hz and amplitude 2.6 mm comparatively with seems indicator of the direct laser deposition with spot diameter 3.2 mm without oscillating. © 2018 IEEE.

Важность темы SciVal

Тема: Laser cladding | Titanium alloys | powder feeding

Процентиль важности: 99.051

Ключевые слова автора

Direct laser deposition | High power fiber laser | Transversal oscillating of laser radiation

Связанные документы

Dynamic beam shaping with polarization control at the image plane for material processing
Tang, Y. , Li, J. , Zhou, T.